PERGAMON

International Journal of Solids and Structures 38 (2001) 91–113

INTERNATIONAL JOURNAL OF SOLIDS and STRUCTURES

www.elsevier.com/locate/ijsolstr

Singular stress fields of angle-ply and monoclinic bimaterial wedges

P. Poonsawat [a], A.C. Wijeyewickrema [b,*], P. Karasudhi [b]

[a] *School of Civil Engineering, Rangsit University, Muang Ake, Pathumthani 12000, Thailand*
[b] *School of Civil Engineering, Asian Institute of Technology, P.O. Box 4, Klong Luang, Pathumthani 12120, Thailand*

Received 20 April 1999

Abstract

The characteristic equations for the order of stress singularity of anisotropic bimaterial wedges subjected to traction boundary conditions are investigated. For an angle-ply bimaterial wedge, both fully bonded and frictional interfaces are considered, whereas for a monoclinic bimaterial wedge, a frictional interface is considered. Here, the Stroh formalism and the separation of variables technique are used. In general, the order of stress singularity can be real or complex, but for the special geometry of a crack along the frictional interface of a monoclinic composite, it is always real. Explicit characteristic equations for the order of singularity are presented for an aligned orthotropic composite with a frictional interface. Numerical results are given for an angle-ply bimaterial wedge and a monoclinic bimaterial wedge consisting of a graphite/epoxy fiber-reinforced composite.

Keywords: Anisotropic; Bimaterial; Composite materials; Frictional interfaces; Singularities

1. Introduction

Anisotropic composites are widely used in many engineering fields due to advantageous properties such as high strength to weight and high stiffness to weight ratios, which are crucial in making structural components more efficient and cost-effective. To supplement experiments, which are conducted to understand the failure mechanisms and to determine damage criteria, rigorous stress analysis of the singular stresses, which occur at the apex of composite wedges, is required. The region very close to the geometric singular point of many practical problems can be considered as either a single-material wedge or a multi-material wedge, e.g., the tip of a crack in a homogeneous body can be modeled as a single-material wedge of angle 2π. Singular stresses at the wedge apex are proportional to r^{-k}, where k is the order of the power singularity and r is the distance from the apex.

The initial studies of stress singularities were limited to two-dimensional problems of elastically isotropic materials. The singular stresses at the apex of a single-material wedge with various boundary conditions were

* Corresponding author. Fax: +662-524-6059.
E-mail address: anilcw@ait.ac.th (A.C. Wijeyewickrema).

0020-7683/00/$ - see front matter
PII: S0020-7683(00)00016-0

first investigated by Williams (1952) and Kalandiia (1969). The singularities for bimaterial wedges consisting of two dissimilar wedges of angle $\pi/2$ with fully bonded interfaces were studied by Bogy (1968, 1970) and the singularities for bimaterial wedges of arbitrary angles were studied by Bogy (1971), Bogy and Wang (1971) and Hein and Erdogan (1971). The singularity of a wedge pressing on a half-plane was studied by Dundurs and Lee (1972) for a slipping interface and by Gdoutos and Theocaris (1975) for the fully bonded and frictional interfaces. The existence of power singularities was investigated by Comninou (1976), and some experimental results in photoelastic tests were given for a wedge in contact with a half-plane with friction. The analysis of singular stress fields at the apex of a multi-material wedge was presented by Dempsey and Sinclair (1979). The three principal methods used in these studies to obtain the order of singularity for two-dimensional problems are: (i) the Airy stress function method in conjunction with the separation of variables method, initially used by Williams (1952); (ii) the complex potential method, initially used by Gdoutos and Theocaris (1975); and (iii) the Mellin integral transform method, initially used by Bogy (1968).

In the case of elastically anisotropic materials, several solution schemes have been proposed. In general, it is not possible to decompose a two-dimensional problem into in-plane and anti-plane problems and the displacements $u_i = u_i(x_1, x_2)$, $i = 1$–3 are non-zero. The earliest scheme of Lekhnitskii (1950) can be considered as the extension of the Airy-stress function method for isotropic material. The method of Eshelby et al. (1953) uses displacement functions with the assumption that all displacement components do not vanish but depend on two Cartesian coordinates, say x_1 and x_2. Hence, the method is applicable only for a two-dimensional problem, i.e., the geometry and the external applied loads do not vary in the x_3 direction. The more restrictive solution technique of Green and Zerna (1954) uses a complex function representation of solutions for anisotropic elastic solids and assumes that the anisotropic material is symmetric with respect to the cross-sectional plane, i.e., the x_1–x_2 plane. This scheme is applicable only for the in-plane problem, namely, plane strain or generalized plane stress. Later, the method of Eshelby et al. was modified in a more elegant manner by Stroh (1958) and is referred to in the literature as the *Stroh formalism*.

The order of singularity for a single-material anisotropic wedge was initially investigated by Bogy (1972) for an orthotropic symmetrical wedge subjected to normal and shear loading, by employing the complex function representation of Green and Zerna in conjunction with the Mellin integral transform method. Using this technique, Kuo and Bogy (1974a) considered an orthotropic symmetrical wedge with displacement and traction-displacement boundaries, and Kuo and Bogy (1974b) considered an orthotropic unsymmetrical wedge and a symmetrically twinned composite wedge. Delale (1984) employed the formulation of Lekhnitskii together with the separation of variables method to investigate the order of singularity for an anisotropic bimaterial wedge. Free-edge singular stresses of layered anisotropic composite wedges under extension were studied by Wang and Choi (1982) and Zwiers et al. (1982), and the possible existence of logarithmic singularities was discussed by the latter. The free-edge singular stress problem was further studied by Kim and Im (1995) for the general case of layered anisotropic composite wedges subjected to a combination of uniaxial tension or compression, pure bending and torsion. Singularities for an anisotropic bimaterial wedge were investigated by Lin and Sung (1998) and detailed results were given for the in-plane problem of aligned orthotropic composites.

For boundary-value problems dealing with complicated shapes, the order of singularity obtained here is important to improve the efficiency of conventional numerical methods such as finite element methods and boundary element methods. Conventional finite element solutions show good agreement with analytic solutions for points away from the singularity point. In certain instances, finite and boundary element methods may provide good agreement with analytic solutions near singular points without incorporating the stress singularities as reported by Szabó and Babuška (1991) and Oh and Babuška (1995). In the region, where stresses are singular, accurate finite element solutions could be obtained by explicitly incorporating the known stress singularities in the finite element codes.

Experimental investigations of layered composites indicate that the bond at the interface may be broken before failure occurs. Hence, in this study, the orders of stress singularity for an anisotropic composite

wedge with either a fully bonded interface or a frictional interface are studied. The frictional interface is assumed to be governed by Coulomb's law of friction. The Stroh formalism and the necessary expressions for displacements and stresses for two-dimensional problems are given in Section 2. The expressions for displacements and stresses in the singular stress analysis of an anisotropic composite wedge are presented in Section 3, by following the work of Ting and Chou (1981) and the characteristic equations to determine the order of singularity are formulated for the cases of fully bonded and frictional interfaces. Here, both faces of the wedge are considered traction-free. The equations for angle-ply bimaterial wedges are too complicated to obtain compact expressions for special cases of geometry. However, detailed analysis is done in Section 4 for the special case of a monoclinic bimaterial wedge with a frictional interface, where the symmetric planes of monoclinic materials coincide with each other and with the cross-sectional plane. Only the problem associated with the in-plane deformation is considered there. The exact order of singularity for a crack along the frictional interface of a monoclinic bimaterial composite is obtained in Section 4.1 and the explicit equation to determine the order of singularity for an aligned orthotropic bimaterial wedge is presented in Section 4.2. In Section 4.3, the special case of an aligned degenerate orthotropic bimaterial wedge is considered. Finally, in Section 5, numerical results for a graphite/epoxy fiber-reinforced composite wedge are presented for two cases: (1) an angle-ply bimaterial wedge, where the fibers in each layer are parallel to the interface and (2) a monoclinic bimaterial wedge, where the fibers in both materials are parallel to the cross-sectional plane.

2. Fundamental equations for anisotropic elastic bodies

For two-dimensional problems in anisotropic elasticity, where all physical quantities depend only on the x_1 and x_2 coordinates of the reference Cartesian coordinate system, the displacement field can be written as

$$u_i(x_1, x_2) = a_i f(x_1 + p x_2), \quad i = 1, 2, 3, \tag{1}$$

where $f(z)$ is an analytic function of the complex variable $z = x_1 + p x_2$ (Stroh, 1958). The constant p is determined from the sextic equation

$$\left| C_{i1k1} + p(C_{i1k2} + C_{i2k1}) + p^2 C_{i2k2} \right| = 0, \tag{2a}$$

and the constants a_i are determined from

$$\left[C_{i1k1} + p(C_{i1k2} + C_{i2k1}) + p^2 C_{i2k2} \right] a_k = 0, \tag{2b}$$

where C_{ijkl} are the elastic stiffnesses and repeated Latin indices imply summation. The elastic constants have the symmetric properties $C_{ijkl} = C_{jikl} = C_{ijlk} = C_{klij}$. Eshelby et al. (1953) have shown that the roots of Eq. (2a) cannot be real. Hence, when all six roots are assumed to be distinct, the three different pairs of complex conjugates are denoted by p_α and $\overline{p}_\alpha$ ($\alpha = 1$–3), where the imaginary part of p_α is taken to be positive and an overbar represents the complex conjugate. The value of a_i corresponding to p_α and $\overline{p}_\alpha$ are denoted by $a_{i\alpha}$ and $\overline{a}_{i\alpha}$, respectively. A general expression for the displacements can then be written as

$$u_i(x_1, x_2) = \sum_{\alpha=1}^{3} [a_{i\alpha} f_\alpha(x_1 + p_\alpha x_2) + \overline{a}_{i\alpha} g_\alpha(x_1 + \overline{p}_\alpha x_2)]. \tag{3}$$

The stress components σ_{ij} are related to the strain components ε_{ij} through Hooke's law, and hence, the stress fields are related to the displacement fields by

$$\sigma_{ij}(x_1, x_2) = C_{ijkl}\varepsilon_{kl} = C_{ijkl} u_{k,l} = \sum_{\alpha=1}^{3} \left[\boldsymbol{\tau}_{ij\alpha} f'_\alpha(x_1 + p_\alpha x_2) + \overline{\boldsymbol{\tau}}_{ij\alpha} g'_\alpha(x_1 + \overline{p}_\alpha x_2) \right], \tag{4}$$

where

$$\tau_{ij\alpha} = (C_{ijk1} + p_\alpha C_{ijk2})a_{k\alpha}. \tag{5}$$

On account of Eqs. (5) and (2b), it is convenient to introduce

$$b_{i\alpha} \equiv \tau_{i2\alpha} = -\frac{1}{p_\alpha}\tau_{i1\alpha} = -\frac{1}{p_\alpha}(C_{i1kl} + p_\alpha C_{i1k2})a_{k\alpha}, \tag{6}$$

and hence, the stress fields can be expressed as

$$\sigma_{i1}(x_1, x_2) = -\sum_{\alpha=1}^{3}[p_\alpha b_{i\alpha} f'_\alpha(x_1 + p_\alpha x_2) + \overline{p}_\alpha \overline{b}_{i\alpha} g'_\alpha(x_1 + \overline{p}_\alpha x_2)], \tag{7a}$$

$$\sigma_{i2}(x_1, x_2) = \sum_{\alpha=1}^{3}\left[b_{i\alpha} f'_\alpha(x_1 + p_\alpha x_2) + \overline{b}_{i\alpha} g'_\alpha(x_1 + \overline{p}_\alpha x_2)\right]. \tag{7b}$$

The expressions for the displacement and stress fields in Eqs. (3), (7a) and (7b) can be obtained in the polar coordinate system (r, θ) by substituting $x_1 = r\cos\theta$ and $x_2 = r\sin\theta$, as

$$u_i(r, \theta) = \sum_{\alpha=1}^{3}\left[a_{i\alpha} f_\alpha(r\zeta_\alpha) + \overline{a}_{i\alpha} g_\alpha(r\overline{\zeta}_\alpha)\right], \tag{8}$$

$$\sigma_{i1}(r, \theta) = -\sum_{\alpha=1}^{3}\left[p_\alpha b_{i\alpha} f'_\alpha(r\zeta_\alpha) + \overline{p}_\alpha \overline{b}_{i\alpha} g'_\alpha(r\overline{\zeta}_\alpha)\right], \tag{9a}$$

$$\sigma_{i2}(r, \theta) = \sum_{\alpha=1}^{3}\left[b_{i\alpha} f'_\alpha(r\zeta_\alpha) + \overline{b}_{i\alpha} g'_\alpha(r\overline{\zeta}_\alpha)\right], \tag{9b}$$

where

$$\zeta_\alpha \equiv \zeta_\alpha(\theta) = \cos\theta + p_\alpha \sin\theta. \tag{10}$$

The traction on a radial plane with a unit outward normal vector $n_j \equiv (-\sin\theta, \cos\theta, 0)$ can be obtained as

$$t_i(r, \theta) = \sigma_{ij} n_j = -\sigma_{i1}\sin\theta + \sigma_{i2}\cos\theta = \sum_{\alpha=1}^{3}\left[\zeta_\alpha b_{i\alpha} f'_\alpha(r\zeta_\alpha) + \overline{\zeta}_\alpha \overline{b}_{i\alpha} g'_\alpha(r\overline{\zeta}_\alpha)\right]. \tag{11}$$

3. Singular stress analysis of an anisotropic composite wedge

The unknown functions $f_\alpha(r\zeta_\alpha)$ and $g_\alpha(r\zeta_\alpha)$ in Eqs. (9a) and (9b) are chosen such that $\sigma_{ij} = r^{-k}F_{ij}(\theta)$, where k is the order of singularity and r is the distance from the wedge apex. The value of k can be either real or complex. When k is complex, the singular stress field is oscillatory and the strength of singularity is dominated by $\mathrm{Re}(k)$. To ensure that the strain energy is bounded everywhere including the region where $r \to 0$, the order of singularity of interest is in the range $0 < \mathrm{Re}(k) < 1$. Following the work of Ting and Chou (1981),

$$f_\alpha(r\zeta_\alpha) = (r\zeta_\alpha)^{1-k} m_\alpha/(1-k), \qquad g_\alpha(r\overline{\zeta}_\alpha) = (r\overline{\zeta}_\alpha)^{1-k} n_\alpha/(1-k), \tag{12}$$

where m_α and n_α are arbitrary constants. Hence, Eqs. (8), (9a), (9b) and (11) can be rewritten as

$$u_i(r,\theta) = r^{1-k}\sum_{\alpha=1}^{3}\left[a_{i\alpha}\zeta_\alpha^{1-k}(\theta)m_\alpha + \overline{a}_{i\alpha}\overline{\zeta}_\alpha^{1-k}(\theta)n_\alpha\right]/(1-k), \tag{13}$$

$$\sigma_{i1}(r,\theta) = -r^{-k}\sum_{\alpha=1}^{3}\left[b_{i\alpha}p_\alpha\zeta_\alpha^{-k}(\theta)m_\alpha + \overline{b}_{i\alpha}\overline{p}_\alpha\overline{\zeta}_\alpha^{-k}(\theta)n_\alpha\right], \tag{14a}$$

$$\sigma_{i2}(r,\theta) = r^{-k}\sum_{\alpha=1}^{3}\left[b_{i\alpha}\zeta_\alpha^{-k}(\theta)m_\alpha + \overline{b}_{i\alpha}\overline{\zeta}_\alpha^{-k}(\theta)n_\alpha\right], \tag{14b}$$

$$t_i(r,\theta) = r^{-k}\sum_{\alpha=1}^{3}\left[b_{i\alpha}\zeta_\alpha^{1-k}(\theta)m_\alpha + \overline{b}_{i\alpha}\overline{\zeta}_\alpha^{1-k}(\theta)n_\alpha\right], \tag{15}$$

or, in the matrix form,

$$\mathbf{u}(r,\theta) = \frac{r^{1-k}}{1-k}\left(\mathbf{A}\langle\zeta_*^{1-k}\rangle\mathbf{m} + \overline{\mathbf{A}}\left\langle\overline{\zeta}_*^{1-k}\right\rangle\mathbf{n}\right), \tag{16}$$

$$\boldsymbol{\sigma}_1(r,\theta) = -r^{-k}\left(\mathbf{B}\langle p_*\zeta_*^{-k}\rangle\mathbf{m} + \overline{\mathbf{B}}\left\langle\overline{p}_*\overline{\zeta}_*^{-k}\right\rangle\mathbf{n}\right), \tag{17a}$$

$$\boldsymbol{\sigma}_2(r,\theta) = r^{-k}\left(\mathbf{B}\langle\zeta_*^{-k}\rangle\mathbf{m} + \overline{\mathbf{B}}\left\langle\overline{\zeta}_*^{-k}\right\rangle\mathbf{n}\right), \tag{17b}$$

$$\mathbf{t}(r,\theta) = r^{-k}\left(\mathbf{B}\langle\zeta_*^{1-k}\rangle\mathbf{m} + \overline{\mathbf{B}}\left\langle\overline{\zeta}_*^{1-k}\right\rangle\mathbf{n}\right), \tag{18}$$

where

$$\begin{aligned}&\mathbf{u} = \{u_i\}, \quad \boldsymbol{\sigma}_1 = \{\sigma_{i1}\}, \quad \boldsymbol{\sigma}_2 = \{\sigma_{i2}\}, \quad \mathbf{t} = \{t_i\},\\ &\mathbf{A} = [a_{i\alpha}], \quad \mathbf{B} = [b_{i\alpha}], \quad \mathbf{m} = \{m_\alpha\}, \quad \mathbf{n} = \{n_\alpha\},\end{aligned} \tag{19}$$

and the angle brackets denote diagonal matrices, i.e.,

$$\left\langle\zeta_*^{-k}\right\rangle = \begin{bmatrix}\zeta_1^{-k} & 0 & 0\\ 0 & \zeta_2^{-k} & 0\\ 0 & 0 & \zeta_3^{-k}\end{bmatrix}, \qquad \left\langle p_*\zeta_*^{-k}\right\rangle = \begin{bmatrix}p_1\zeta_1^{-k} & 0 & 0\\ 0 & p_2\zeta_2^{-k} & 0\\ 0 & 0 & p_3\zeta_3^{-k}\end{bmatrix}. \tag{20}$$

Here, the unknown vectors $\mathbf{m}$ and $\mathbf{n}$ can be determined from given boundary conditions. Since the matrices $\mathbf{A}$ and $\mathbf{B}$ are not singular when p_α are distinct (Stroh, 1958), for convenience, in the formulation $\mathbf{m}$ and $\mathbf{n}$ can be replaced by $\mathbf{B}^{-1}\mathbf{m}$ and $\overline{\mathbf{B}}^{-1}\mathbf{n}$, respectively. Then, it follows from Eqs. (16)–(18) that

$$\mathbf{u}(r,\theta) = -i\frac{r^{1-k}}{1-k}\left(\mathbf{M}^{-1}\mathbf{B}\langle\zeta_*^{1-k}\rangle\mathbf{B}^{-1}\mathbf{m} - \overline{\mathbf{M}}^{-1}\overline{\mathbf{B}}\left\langle\overline{\zeta}_*^{1-k}\right\rangle\overline{\mathbf{B}}^{-1}\mathbf{n}\right), \tag{21}$$

$$\boldsymbol{\sigma}_1(r,\theta) = -r^{-k}\left(\mathbf{B}\langle p_*\zeta_*^{-k}\rangle\mathbf{B}^{-1}\mathbf{m} + \overline{\mathbf{B}}\left\langle\overline{p}_*\overline{\zeta}_*^{-k}\right\rangle\overline{\mathbf{B}}^{-1}\mathbf{n}\right), \tag{22a}$$

$$\boldsymbol{\sigma}_2(r,\theta) = r^{-k}\left(\mathbf{B}\langle\zeta_*^{-k}\rangle\mathbf{B}^{-1}\mathbf{m} + \overline{\mathbf{B}}\left\langle\overline{\zeta}_*^{-k}\right\rangle\overline{\mathbf{B}}^{-1}\mathbf{n}\right), \tag{22b}$$

$$\mathbf{t}(r,\theta) = r^{-k}\left(\mathbf{B}\langle\zeta_*^{1-k}\rangle\mathbf{B}^{-1}\mathbf{m} + \overline{\mathbf{B}}\left\langle\overline{\zeta}_*^{1-k}\right\rangle\overline{\mathbf{B}}^{-1}\mathbf{n}\right). \tag{23}$$

The equations corresponding to the situation when p_α are not distinct were studied by Ting and Chou (1981). In Eq. (21), the impedance matrix $\mathbf{M}$ and its inverse are defined by

$$\mathbf{M} = -i\mathbf{B}\mathbf{A}^{-1} = \mathbf{H}^{-1} + i\mathbf{H}^{-1}\mathbf{S}, \qquad \mathbf{M}^{-1} = i\mathbf{A}\mathbf{B}^{-1} = \mathbf{L}^{-1} - i\mathbf{S}\mathbf{L}^{-1}, \tag{24}$$

where the matrices $\mathbf{H}$ and $\mathbf{L}$ are symmetric and positive definite but $\mathbf{H}^{-1}\mathbf{S}$ and $\mathbf{S}\mathbf{L}^{-1}$ are skew-symmetric. The matrices $\mathbf{H}$, $\mathbf{L}$ and $\mathbf{S}$ were first introduced by Barnett and Lothe (1973), who showed that these matrices were real. These matrices are discussed extensively by Ting (1996, Chapters 5–6).

3.1. An anisotropic bimaterial wedge with a fully bonded interface

The bimaterial wedge shown in Fig. 1 consists of two wedges with wedge angles θ_1 and θ_2 joined together along the interface, which is the x_1–x_3 plane. The upper wedge occupies the domain $0 \leqslant \theta \leqslant \theta_1$, whereas the lower wedge occupies the domain $-\theta_2 \leqslant \theta \leqslant 0$. Superscripts or subscripts (1) and (2) are used to denote the quantities associated with the upper wedge and the lower wedge, respectively.

The traction-free boundary conditions at the wedge faces are

$$t_i^{(1)}(r, \theta_1) = 0, \quad t_i^{(2)}(r, -\theta_2) = 0 \qquad (i = 1, 2, 3). \tag{25}$$

Making use of Eq. (25), the expressions for displacements and tractions in Eqs. (21) and (23) can be written for different regions as follows:

for the upper wedge 1, i.e., $0 \leqslant \theta \leqslant \theta_1$:

$$\mathbf{u}^{(1)}(r, \theta) = -i\frac{r^{1-k}}{1-k}\left(\mathbf{M}_{(1)}^{-1}\mathbf{\Gamma}_{(1)}(\theta, k)\mathbf{\Omega}_{(1)}(k) + \overline{\mathbf{M}}_{(1)}^{-1}\overline{\mathbf{\Gamma}}_{(1)}(\theta, k)\overline{\mathbf{\Omega}}_{(1)}(k)\right)\mathbf{m}^{(1)}, \tag{26a}$$

$$\mathbf{t}^{(1)}(r, \theta) = r^{-k}\left(\mathbf{\Gamma}_{(1)}(\theta, k)\mathbf{\Omega}_{(1)}(k) - \overline{\mathbf{\Gamma}}_{(1)}(\theta, k)\overline{\mathbf{\Omega}}_{(1)}(k)\right)\mathbf{m}^{(1)}; \tag{26b}$$

for the lower wedge 2, i.e., $-\theta_2 \leqslant \theta \leqslant 0$:

$$\mathbf{u}^{(2)}(r, \theta) = -i\frac{r^{1-k}}{1-k}\left(\mathbf{M}_{(2)}^{-1}\mathbf{\Gamma}_{(2)}(\theta, k)\mathbf{\Omega}_{(2)}(k) + \overline{\mathbf{M}}_{(2)}^{-1}\overline{\mathbf{\Gamma}}_{(2)}(\theta, k)\overline{\mathbf{\Omega}}_{(2)}(k)\right)\mathbf{m}^{(2)}, \tag{27a}$$

$$\mathbf{t}^{(2)}(r, \theta) = r^{-k}\left(\mathbf{\Gamma}_{(2)}(\theta, k)\mathbf{\Omega}_{(2)}(k) - \overline{\mathbf{\Gamma}}_{(2)}(\theta, k)\overline{\mathbf{\Omega}}_{(2)}(k)\right)\mathbf{m}^{(2)}, \tag{27b}$$

where

$$\mathbf{\Gamma}_{(N)}(\theta, k) = \mathbf{B}_{(N)}\left\langle \zeta_{*(N)}^{1-k}(\theta)\right\rangle \mathbf{B}_{(N)}^{-1} \quad (N = 1, 2) \tag{28a}$$

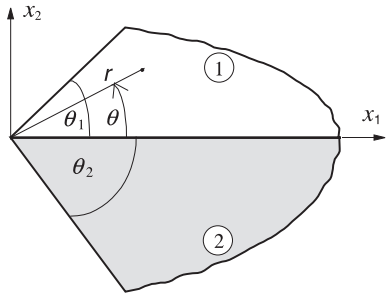

Fig. 1. A bimaterial anisotropic composite wedge.

$$\mathbf{\Omega}_{(1)}(k) = \left(\mathbf{\Gamma}_{(1)}(\theta_1, k)\right)^{-1}, \tag{28b}$$

$$\mathbf{\Omega}_{(2)}(k) = \left(\mathbf{\Gamma}_{(2)}(-\theta_2, k)\right)^{-1}. \tag{28c}$$

The continuity of tractions and displacements along the fully bonded interface are given by

$$t_i^{(1)}(r,0) = t_i^{(2)}(r,0), \qquad u_i^{(1)}(r,0) = u_i^{(2)}(r,0). \tag{29}$$

Substituting Eqs. (26a), (26b) and (27a), (27b) into Eq. (29) results in

$$\left(\mathbf{\Omega}_{(1)}(k) - \overline{\mathbf{\Omega}}_{(1)}(k)\right)\mathbf{m}^{(1)} = \left(\mathbf{\Omega}_{(2)}(k) - \overline{\mathbf{\Omega}}_{(2)}(k)\right)\mathbf{m}^{(2)}, \tag{30}$$

$$\left(\mathbf{M}_{(1)}^{-1}\mathbf{\Omega}_{(1)}(k) + \overline{\mathbf{M}}_{(1)}^{-1}\overline{\mathbf{\Omega}}_{(1)}(k)\right)\mathbf{m}^{(1)} = \left(\mathbf{M}_{(2)}^{-1}\mathbf{\Omega}_{(2)}(k) + \overline{\mathbf{M}}_{(2)}^{-1}\overline{\mathbf{\Omega}}_{(2)}(k)\right)\mathbf{m}^{(2)}. \tag{31}$$

Eliminating $\mathbf{m}^{(1)}$ from Eqs. (30) and (31), and making use of Eq. (24) yields

$$\left[\mathbf{K}(k) - \overline{\mathbf{K}}(k)\right]\mathbf{m}^{(2)} = \mathbf{0}, \tag{32}$$

where

$$\mathbf{K}(k) = [\mathbf{\Omega}_{(1)}(k)]^{-1}\mathbf{L}_{(1)}\left(\overline{\mathbf{M}}_{(1)}^{-1} + \mathbf{M}_{(2)}^{-1}\right)\mathbf{\Omega}_{(2)}(k) + [\overline{\mathbf{\Omega}}_{(1)}(k)]^{-1}\mathbf{L}_{(1)}\left(\mathbf{M}_{(1)}^{-1} - \mathbf{M}_{(2)}^{-1}\right)\mathbf{\Omega}_{(2)}(k). \tag{33}$$

The characteristic equation to determine k is given by

$$\left|\mathbf{K}(k) - \overline{\mathbf{K}}(k)\right| = 0. \tag{34}$$

It can be shown that Eq. (34) agrees with that obtained by Lin and Sung (1998), who also presented an explicit expression for Eq. (34) for the in-plane deformation of aligned orthotropic bimaterial wedges.

The roots of Eq. (34) depend on the wedge angles θ_1 and θ_2 and elastic constants of both wedges. For the special case of a crack in a homogeneous material, i.e., $\theta_1 = \theta_2 = \pi$ and wedges 1 and 2 consist of the same anisotropic material; $k = 0.5$ of multiplicity 3 (Ting, 1986). For an interface crack, i.e., $\theta_1 = \theta_2 = \pi$ but wedges 1 and 2 consist of different anisotropic materials, $k = 0.5$ and $0.5 \pm \varsigma i$, where the positive constant ς depends on material constants of both wedges (Ting, 1986; Suo, 1990). The singular stress corresponding to repeated values of k, which may result in a logarithmic singularity was studied by Ting and Chou (1981). For other geometries, the roots of k cannot be obtained in a closed form.

3.2. An anisotropic bimaterial wedge with a frictional interface

Two cases associated with the upper wedge slipping to the right and to the left relative to the lower wedge need to be considered (Fig. 2). However, both cases are formulated at the same time by allowing the coefficient of friction μ, to be either positive or negative. Positive values of μ correspond to the case when the upper wedge slips to the right relative to the lower wedge and negative values of μ correspond to the case when the upper wedge slips to the left relative to the lower wedge.

At the wedge faces, the traction-free conditions in Eq. (25) are identically satisfied by the expressions for displacements and tractions given in Eqs. (26a), (26b) and (27a), (27b). At the frictional interface $\theta = 0$, the continuity of tractions are given by Eq. (30). The continuity of displacements in x_2 and x_3 directions and Coulomb's law of friction are given by

$$u_2^{(1)}(r,0) = u_2^{(2)}(r,0), \qquad u_3^{(1)}(r,0) = u_3^{(2)}(r,0), \qquad \sigma_{21}^{(1)}(r,0) = -\mu\sigma_{22}^{(1)}(r,0), \tag{35}$$

where it is assumed that $\sigma_{22}^{(1)}(r,0) < 0$. Substituting Eqs. (26a), (26b) and (27a), (27b) into Eq. (35) results in

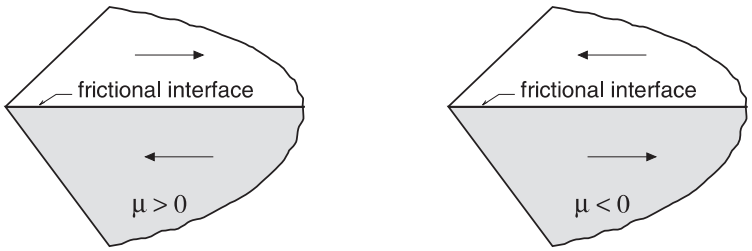

Fig. 2. Configurations of two relative slip directions: (a) the upper wedge slipping to the right relative to the lower wedge and (b) the upper wedge slipping to the left relative to the lower wedge.

$$\left(\left(\mathbf{D}\mathbf{M}_{(1)}^{-1}+\mathbf{C}\right)\mathbf{\Omega}_{(1)}(k)+\left(\mathbf{D}\overline{\mathbf{M}}_{(1)}^{-1}-\mathbf{C}\right)\overline{\mathbf{\Omega}}_{(1)}(k)\right)\mathbf{m}^{(1)}=\left(\mathbf{D}\mathbf{M}_{(2)}^{-1}\mathbf{\Omega}_{(2)}(k)+\mathbf{D}\overline{\mathbf{M}}_{(2)}^{-1}\overline{\mathbf{\Omega}}_{(2)}(k)\right)\mathbf{m}^{(2)}, \tag{36}$$

where

$$\mathbf{C}=\begin{bmatrix}1 & \mu & 0\\ 0 & 0 & 0\\ 0 & 0 & 0\end{bmatrix},\qquad \mathbf{D}=\begin{bmatrix}0 & 0 & 0\\ 0 & 1 & 0\\ 0 & 0 & 1\end{bmatrix}. \tag{37}$$

Eqs. (30) and (36) can be written in the matrix form as

$$\mathbf{K}^{f}(k)\mathbf{g}=\mathbf{0}, \tag{38}$$

where the 6×6 matrix $\mathbf{K}^{f}(k)$ is given by

$$\mathbf{K}^{f}(k)=\begin{bmatrix}\mathbf{\Omega}_{(1)}(k)-\overline{\mathbf{\Omega}}_{(1)}(k) & \mathbf{\Omega}_{(2)}(k)-\overline{\mathbf{\Omega}}_{(2)}(k)\\ \left(\mathbf{D}\mathbf{M}_{(1)}^{-1}+\mathbf{C}\right)\mathbf{\Omega}_{(1)}(k)+\left(\mathbf{D}\overline{\mathbf{M}}_{(1)}^{-1}-\mathbf{C}\right)\overline{\mathbf{\Omega}}_{(1)}(k) & \mathbf{D}\mathbf{M}_{(2)}^{-1}\mathbf{\Omega}_{(2)}(k)+\mathbf{D}\overline{\mathbf{M}}_{(2)}^{-1}\overline{\mathbf{\Omega}}_{(2)}(k)\end{bmatrix}, \tag{39}$$

and $\mathbf{g}=\left\{m_1^{(1)},m_2^{(1)},m_3^{(1)},-m_1^{(2)},-m_2^{(2)},-m_3^{(2)}\right\}^{\mathrm{T}}$. The order of singularity is determined by the condition that

$$\left|\mathbf{K}^{f}(k)\right|=0. \tag{40}$$

4. A monoclinic bimaterial wedge with a frictional interface

A bimaterial wedge consisting of dissimilar monoclinic materials is considered, where the symmetrical planes of the monoclinic materials coincide with the plane $x_3=0$ of the Cartesian coordinate system. As a result, the in-plane and anti-plane deformation is uncoupled and only the order of singularity associated with the in-plane deformation is studied. The order of singularity for a monoclinic bimaterial wedge with a frictional interface can be obtained by solving Eq. (40); however, the size of the characteristic matrix $\mathbf{K}^{f}$ corresponding to the in-plane deformation reduces from 6×6 to 4×4. Hence, now all matrices on the right-hand side of Eq. (39) are 2×2 matrices. Instead of using Eq. (2a) to determine the complex parameters p_1 and p_2 corresponding to the in-plane deformation, the quartic equation, which is more compact (Lekhnitskii, 1950, Eq. (22.6)),

$$s'_{11}p^4-2s'_{16}p^3+(2s'_{12}+s'_{66})p^2-2s'_{26}p+s'_{22}=0 \tag{41}$$

can be used. Here, s'_{mn} are the reduced elastic compliances defined by

$$s'_{mn} = s_{mn} - \frac{s_{m3}s_{3n}}{s_{33}} \tag{42}$$

and s_{mn} are the elastic compliances. The matrices **A** and **B** defined in Eq. (19) are now given by

$$\mathbf{A} = \begin{bmatrix} \xi(p_1) & \xi(p_2) \\ \eta(p_1) & \eta(p_2) \end{bmatrix}, \qquad \mathbf{B} = \begin{bmatrix} -p_1 & -p_2 \\ 1 & 1 \end{bmatrix}, \tag{43}$$

where

$$\xi(p) = s'_{11}p^2 - s'_{16}p + s'_{12}, \qquad \eta(p) = s'_{12}p - s'_{26} + s'_{22}p^{-1}. \tag{44}$$

The expression for $\mathbf{M}^{-1}$ is obtained by substituting Eq. (43) into Eq. (24) and making use of Eq. (41), and hence, $\mathbf{L}^{-1}$ and $\mathbf{SL}^{-1}$ are obtained as

$$\mathbf{L}^{-1} = s'_{11}\mathbf{P}, \qquad \mathbf{SL}^{-1} = \omega\mathbf{J}, \tag{45}$$

where

$$\mathbf{P} = \begin{bmatrix} b & d \\ d & e \end{bmatrix}, \qquad \mathbf{J} = \begin{bmatrix} 0 & -1 \\ 1 & 0 \end{bmatrix}, \tag{46}$$

$$\omega = s'_{12} - s'_{11}\,\mathrm{Re}(p_1p_2) > 0, \qquad b = \mathrm{Im}(p_1 + p_2) > 0, \tag{47}$$

$$d = \mathrm{Im}(p_1p_2), \qquad e = \mathrm{Im}[p_1p_2(\overline{p}_1 + \overline{p}_2)] > 0. \tag{48}$$

The matrices **C** and **D** in Eq. (37) and $\left\langle \zeta^{1-k}_{*(N)}(\theta) \right\rangle$ in Eq. (28a) are replaced by

$$\mathbf{C} = \begin{bmatrix} 1 & \mu \\ 0 & 0 \end{bmatrix}, \qquad \mathbf{D} = \begin{bmatrix} 0 & 0 \\ 0 & 1 \end{bmatrix}, \qquad \left\langle \zeta^{1-k}_{*(N)}(\theta) \right\rangle = \begin{bmatrix} \zeta^{1-k}_{1(N)}(\theta) & 0 \\ 0 & \zeta^{1-k}_{2(N)}(\theta) \end{bmatrix}, \tag{49}$$

and the matrices $\mathbf{\Omega}_{(N)}(k)$ are obtained by substituting Eqs. (43) and (49) into Eqs. (28a) and (28b).

4.1. An interface crack along the frictional interface of a monoclinic composite

An interface crack corresponds to the case $\theta_1 = \theta_2 = \pi$. Expressions for $\mathbf{\Omega}_{(1)}(k)$ and $\mathbf{\Omega}_{(2)}(k)$ are obtained from Eqs. (28b) and (28c) as

$$\mathbf{\Omega}_{(1)}(k) = \overline{\mathbf{\Omega}}_{(2)}(k) = -\mathrm{e}^{i\pi k}\mathbf{I}, \qquad \mathbf{\Omega}_{(2)}(k) = \overline{\mathbf{\Omega}}_{(1)}(k) = -\mathrm{e}^{-i\pi k}\mathbf{I}. \tag{50}$$

From Eqs. (50), (39) and (40),

$$(\mathrm{e}^{i\pi k} - \mathrm{e}^{-i\pi k})^2 \left| \left[\mathbf{D}\left(\mathbf{M}^{-1}_{(1)} + \overline{\mathbf{M}}^{-1}_{(2)} \right) + \mathbf{C} \right] \mathrm{e}^{i\pi k} + \left[\mathbf{D}\left(\overline{\mathbf{M}}^{-1}_{(1)} + \mathbf{M}^{-1}_{(2)} \right) - \mathbf{C} \right] \mathrm{e}^{-i\pi k} \right| = 0. \tag{51}$$

Substituting Eqs. (49), (24) and (45) into Eq. (51) results in the characteristic equation

$$\sin^4 \pi k \left(F \cot \pi k - (\omega^{(1)} - \omega^{(2)})\mu \right) = 0, \tag{52}$$

where

$$F = s'^{(1)}_{11}(e^{(1)} - \mu d^{(1)}) + s'^{(2)}_{11}(e^{(2)} - \mu d^{(2)}). \tag{53}$$

The roots of Eq. (52) satisfying the condition $0 < \mathrm{Re}(k) < 1$ is obtained as

$$k = 0.5 - \pi^{-1} \arctan(\mu\beta), \quad -\pi/2 < \arctan(\mu\beta) < \pi/2, \tag{54}$$

where

$$\beta = (\omega^{(1)} - \omega^{(2)})/F. \tag{55}$$

For isotropic composites, β in Eq. (55) reduces to the Dundurs constant β and k in Eq. (54) agrees with the results of Gdoutos and Theocaris (1975, Eq. (10)). In contrast to a fully bonded interface, the order of singularity for an interface crack along a frictional interface is real.

4.2. An orthotropic bimaterial wedge with a frictional interface

For an orthotropic material with the symmetry planes of orthotropy coinciding with the Cartesian coordinate planes, $s'_{16} = s'_{26} = 0$ and hence from Eq. (41) the complex parameters p_1 and p_2 associated with the in-plane deformation satisfy

$$s'_{11}p^4 + (2s'_{12} + s'_{66})p^2 + s'_{22} = 0. \tag{56}$$

As discussed in Section 2, the roots p cannot be real. Hence, there are four purely imaginary roots or two pairs of complex conjugates, and the roots with positive imaginary parts have two possible forms,

$$p_\alpha = \rho_\alpha i \quad (\alpha = 1, 2) \quad \text{and} \quad p_1 = \rho_1 + \rho_2 i, \quad p_2 = -\rho_1 + \rho_2 i, \tag{57}$$

where both ρ_1 and ρ_2 are positive. Only the first form is considered in this study. From Eq. (48), $d = 0$. Following the work of Ting (1995), the generalized Dundurs constants α and β for an orthotropic composite are chosen as

$$\alpha = \frac{s'^{(1)}_{11}e^{(1)} - s'^{(2)}_{11}e^{(2)}}{s'^{(1)}_{11}e^{(1)} + s'^{(2)}_{11}e^{(2)}}, \quad \beta = \frac{\omega^{(1)} - \omega^{(2)}}{s'^{(1)}_{11}e^{(1)} + s'^{(2)}_{11}e^{(2)}}. \tag{58}$$

By substituting Eq. (43) into Eqs. (28b) and (28c) and making use of Eq. (57), elements of $\mathbf{\Omega}_{(N)}(k)$ can be expressed as

$$\begin{aligned}
\mathbf{\Omega}^{11}_{(N)}(k) &= R^{-m}_{2(N)}\left[\exp\left(-m\hat{\theta}^{(N)}_2\right) - i\rho^{(N)}_1 A_{(N)} + \rho^{(N)}_1 B_{(N)}\right],\\
\mathbf{\Omega}^{12}_{(N)}(k) &= R^{-m}_{2(N)}\left[\rho^{(N)}_1\rho^{(N)}_2(A_{(N)} + iB_{(N)})\right],\\
\mathbf{\Omega}^{21}_{(N)}(k) &= R^{-m}_{2(N)}(A_{(N)} + iB_{(N)}),\\
\mathbf{\Omega}^{22}_{(N)}(k) &= R^{-m}_{2(N)}\left[\exp\left(-m\hat{\theta}^{(N)}_2\right) + i\rho^{(N)}_2 A_{(N)} - \rho^{(N)}_2 B_{(N)}\right],
\end{aligned} \tag{59}$$

where

$$\begin{aligned}
A_{(N)} &= \left(R^{-m}_{2(N)}\sin m\hat{\theta}^{(N)}_2 - R^{-m}_{1(N)}\sin m\hat{\theta}^{(N)}_1\right)\Big/\left(R^{-m}_{2(N)}\left(\rho^{(N)}_2 - \rho^{(N)}_1\right)\right),\\
B_{(N)} &= \left(R^{-m}_{2(N)}\cos m\hat{\theta}^{(N)}_2 - R^{-m}_{1(N)}\cos m\hat{\theta}^{(N)}_1\right)\Big/\left(R^{-m}_{2(N)}\left(\rho^{(N)}_2 - \rho^{(N)}_1\right)\right),\\
R_{\alpha(N)} &= \left(\cos^2\theta_N + \left(\rho^{(N)}_\alpha\right)^2\sin^2\theta_N\right)^{1/2}, \quad m = 1 - k,\\
\hat{\theta}^{(1)}_\alpha &= \tan^{-1}\left(\rho^{(1)}_\alpha\tan\theta_1\right), \quad \hat{\theta}^{(2)}_\alpha = -\tan^{-1}(\rho^{(2)}_\alpha\tan\theta_2).
\end{aligned} \tag{60}$$

By substituting Eqs. (24), (45), (49) and (59) into Eq. (40) and making use of Eq. (39), the characteristic equation to determine k for an orthotropic bimaterial wedge is expressed as

$$(1+\alpha)P_1^{(2)}P_2^{(1)} - (1-\alpha)P_1^{(1)}P_2^{(2)} + \mu\Big[(1+\alpha)P_1^{(2)}P_3^{(1)} - (1-\alpha)P_1^{(1)}P_3^{(2)} - 2\beta P_1^{(1)}P_1^{(2)}\Big] = 0, \tag{61}$$

where

$$P_1^{(N)} = \left(A_{(N)}^2 + B_{(N)}^2\right)\rho_1^{(N)}\rho_2^{(N)} + A_{(N)}\left(\rho_2^{(N)} - \rho_1^{(N)}\right)\sin m\hat{\theta}_2^{(N)} - \sin^2 m\hat{\theta}_2^{(N)},$$

$$P_2^{(N)} = A_{(N)}\rho_1^{(N)}\cos m\hat{\theta}_2^{(N)} - B_{(N)}\rho_2^{(N)}\sin m\hat{\theta}_2^{(N)} + \cos m\hat{\theta}_2^{(N)}\sin m\hat{\theta}_2^{(N)},$$

$$P_3^{(N)} = \left(A_{(N)}^2 + B_{(N)}^2\right)\rho_2^{(N)} - A_{(N)}\sin m\hat{\theta}_2^{(N)} - B_{(N)}\cos m\hat{\theta}_2^{(N)}. \tag{62}$$

For the special case of an orthotropic wedge pressing on an orthotropic half-plane, by setting $\theta_2 = \pi$ in Eqs. (60) and (62),

$$A_{(2)} = B_{(2)} = 0, \qquad R_{1\,(2)} = R_{2\,(2)} = 1, \qquad \hat{\theta}_1^{(2)} = \hat{\theta}_2^{(2)} = -\pi,$$

$$P_1^{(2)} = -\sin^2 m\pi, \qquad P_2^{(2)} = -\cos m\pi \sin m\pi, \qquad P_3^{(2)} = 0, \tag{63}$$

and the characteristic equation (61) becomes

$$\sin m\pi\Big\{(1-\alpha)P_1^{(1)}\cos m\pi - (1+\alpha)\sin m\pi P_2^{(1)} - \mu\sin m\pi\Big[(1+\alpha)P_3^{(1)} - 2\beta P_1^{(1)}\Big]\Big\} = 0. \tag{64}$$

Further, when the lower half-plane is rigid, the elastic compliance of material 2 is taken to be proportional to the elastic compliance of the material 1,

$$s_{ij}'^{(2)} = \lambda s_{ij}'^{(1)}, \tag{65}$$

where the positive number $\lambda \to 0$. In view of Eq. (58), $\alpha \to 1$ and the limiting value of β is $\omega^{(1)}/s_{11}'^{(1)}e^{(1)}$. It follows from Eq. (64) that

$$-2\sin^2 m\pi\Big\{P_2^{(1)} + \mu\Big(P_3^{(1)} - \beta P_1^{(1)}\Big)\Big\} = 0. \tag{66}$$

4.3. A degenerate orthotropic bimaterial wedge with a frictional interface

The expressions in Eqs. (60) and (62) are specialized for *degenerate* orthotropic materials as follows: if material 1 is degenerate with $\rho_1^{(1)} = \rho_2^{(1)} = \rho^{(1)}$,

$$\hat{\theta}_1^{(1)} = \hat{\theta}_2^{(1)} = \tan^{-1}(\rho^{(1)}\tan\theta_1) = \hat{\theta}^{(1)},$$

$$A_{(1)} = m\cos(m+1)\hat{\theta}^{(1)}\sin\hat{\theta}^{(1)}/\rho^{(1)},$$

$$B_{(1)} = -m\sin(m+1)\hat{\theta}^{(1)}\sin\hat{\theta}^{(1)}/\rho^{(1)},$$

$$P_1^{(1)} = m^2\sin^2\hat{\theta}^{(1)} - \sin^2 m\hat{\theta}^{(1)},$$

$$P_2^{(1)} = \left(m\sin 2\hat{\theta}^{(1)} + \sin 2m\hat{\theta}^{(1)}\right)\Big/2,$$

$$P_3^{(1)} = m(1+m)\sin^2\hat{\theta}^{(1)}/\rho^{(1)}; \tag{67}$$

if material 2 is degenerate with $\rho_1^{(2)} = \rho_2^{(2)} = \rho^{(2)}$,

$$\hat{\theta}_1^{(2)} = \hat{\theta}_2^{(2)} = -\tan^{-1}(\rho^{(2)} \tan\theta_2) = \hat{\theta}^{(2)},$$

$$A_{(2)} = m\cos(m+1)\hat{\theta}^{(2)} \sin\hat{\theta}^{(2)}/\rho^{(2)},$$

$$B_{(2)} = -m\sin(m+1)\hat{\theta}^{(2)} \sin\hat{\theta}^{(2)}/\rho^{(2)},$$

$$P_1^{(2)} = m^2\sin^2\hat{\theta}^{(2)} - \sin^2 m\hat{\theta}^{(2)},$$

$$P_2^{(2)} = \left(m\sin 2\hat{\theta}^{(2)} + \sin 2m\hat{\theta}^{(2)}\right)\Big/2,$$

$$P_3^{(2)} = m(1+m)\sin^2\hat{\theta}^{(2)}/\rho^{(2)}. \tag{68}$$

For the special case of a degenerate orthotropic wedge pressing on a non-degenerate orthotropic half-plane, the characteristic equation is obtained by using Eqs. (64) and (67) as

$$\Big\{2(1-\alpha)(m^2\sin^2\hat{\theta}^{(1)} - \sin^2 m\hat{\theta}^{(1)})\cos m\pi - (1+\alpha)(m\sin 2\hat{\theta}^{(1)} + \sin 2m\hat{\theta}^{(1)})\sin m\pi$$
$$- 2\hat{\mu}\sin m\pi\Big[(1+\alpha)m(1+m)\sin^2\hat{\theta}^{(1)} - 2\hat{\beta}(m^2\sin^2\hat{\theta}^{(1)} - \sin^2 m\hat{\theta}^{(1)})\Big]\Big\}(\sin m\pi)/2 = 0, \tag{69}$$

where

$$\hat{\beta} = \beta\rho^{(1)}, \quad \hat{\mu} = \mu/\rho^{(1)}. \tag{70}$$

Some numerical results for an isotropic wedge in contact with an orthotropic half-plane and for a degenerate orthotropic wedge in contact with a degenerate orthotropic half-plane have been reported by Poonsawat et al. (1998).

Further, when both materials 1 and 2 are isotropic elastic, $\rho^{(1)} = 1$ and, from Eqs. (67) and (70), $\hat{\theta}^{(1)} = \theta_1$, $\hat{\mu} = \mu$, $\hat{\beta} = \beta$. In addition, the generalized Dundurs constants α and β defined by Eqs. (58) reduce to the Dundurs constants α and β. It can be readily shown that Eq. (69) agrees with Eq. (8) of Gdoutos and Theocaris (1975) for the special case of an isotropic wedge pressing on an isotropic half-plane.

5. Numerical results and discussion

For the numerical computations, a graphite/epoxy fiber-reinforced composite, with the elastic constants

$$E_1 = 20 \times 10^6\,\text{psi}, \qquad E_2 = E_3 = 2.1 \times 10^6\,\text{psi},$$

$$G_{12} = G_{23} = G_{13} = 0.85 \times 10^6\,\text{psi}, \tag{71}$$

$$v_{12} = v_{23} = v_{13} = 0.21$$

is taken from Ting and Hoang (1984). Here, E_i, G_{ij} and v_{ij} are the Young modulus, the shear modulus and Poisson's ratio, respectively. The elastic compliance matrix s_{mn}^* is given by

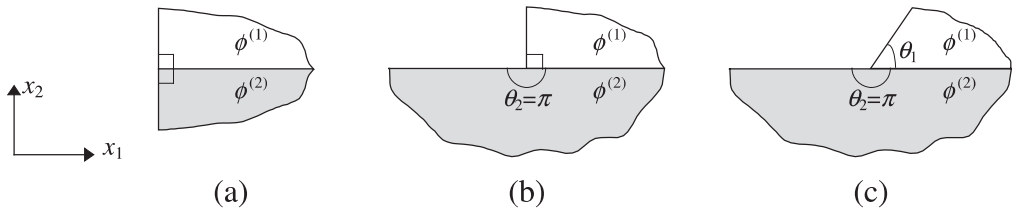

Fig. 3. Wedge configurations considered for numerical analysis of angle-ply bimaterial wedge (or monoclinic bimaterial wedge): (a) the free-edge of a laminate (or two quarter planes pressing against each other) (b) the 90° broken laminate (or a quarter plane pressing on the half-plane) and (c) the inclined broken laminate (or a wedge pressing on the half-plane).

$$\left[s^*_{mn}\right] = \begin{bmatrix} 1/E_1 & -\nu_{12}/E_1 & -\nu_{13}/E_1 & 0 & 0 & 0 \\ -\nu_{12}/E_1 & 1/E_2 & -\nu_{23}/E_2 & 0 & 0 & 0 \\ -\nu_{13}/E_1 & -\nu_{23}/E_3 & 1/E_3 & 0 & 0 & 0 \\ 0 & 0 & 0 & 1/G_{23} & 0 & 0 \\ 0 & 0 & 0 & 0 & 1/G_{13} & 0 \\ 0 & 0 & 0 & 0 & 0 & 1/G_{12} \end{bmatrix}, \tag{72}$$

(Christensen, 1979, pp. 154), and the stiffness matrix C^*_{mn} is obtained by inverting the s^*_{mn} matrix.

For numerical computations, two kinds of composite wedges are considered. The first type of composite wedge is an angle-ply bimaterial wedge with either a fully bonded or frictional interface, where the fibers are parallel to the interface. The three particular geometries considered are shown in Fig. 3, viz, the free-edge of a laminate, the broken laminate and the inclined broken laminate. The second type of composite wedge is a monoclinic bimaterial wedge with a frictional interface, where the fibers are parallel to the cross-sectional plane. Here too, the particular geometries considered are shown in Fig. 3, viz, two quarter planes pressing against each other, a quarter plane pressing on the half-plane and a wedge pressing on the half-plane.

5.1. An angle-ply bimaterial wedge

The local coordinate system (x^*_1, x^*_2, x^*_3) is selected in such a way that the x^*_1-axis is in the longitudinal direction of the fibers. The x^*_2-axis is normal to the layer and coincides with the x_2-axis of the global coordinate system (x_1, x_2, x_3), as shown in Fig. 4. Alternate layers of the wedge have the same fiber orientation. The stiffness matrix $C^{(N)}_{mn}$, $N = 1, 2$, referred to the global coordinate system, is obtained by transforming the stiffness matrix C^*_{mn} according to the ply-angle. The ply-angles of adjacent layers are $\phi^{(1)}$ and $\phi^{(2)}$. For the $\phi^{(N)}$-layer, the global coordinates are related to the local coordinates by

$$\begin{Bmatrix} x_1 \\ x_2 \\ x_3 \end{Bmatrix} = \begin{bmatrix} \cos\phi^{(N)} & 0 & \sin\phi^{(N)} \\ 0 & 1 & 0 \\ -\sin\phi^{(N)} & 0 & \cos\phi^{(N)} \end{bmatrix} \begin{Bmatrix} x^*_1 \\ x^*_2 \\ x^*_3 \end{Bmatrix}, \quad N = 1, 2. \tag{73}$$

The stiffness matrices $C^{(N)}_{mn}$ and C^*_{mn} are related by

$$\left[C^{(N)}\right] = [m][C^*][m]^{\mathrm{T}}, \tag{74}$$

(Auld, 1973, pp. 79–80), where the superscript T denotes the transpose of a matrix and

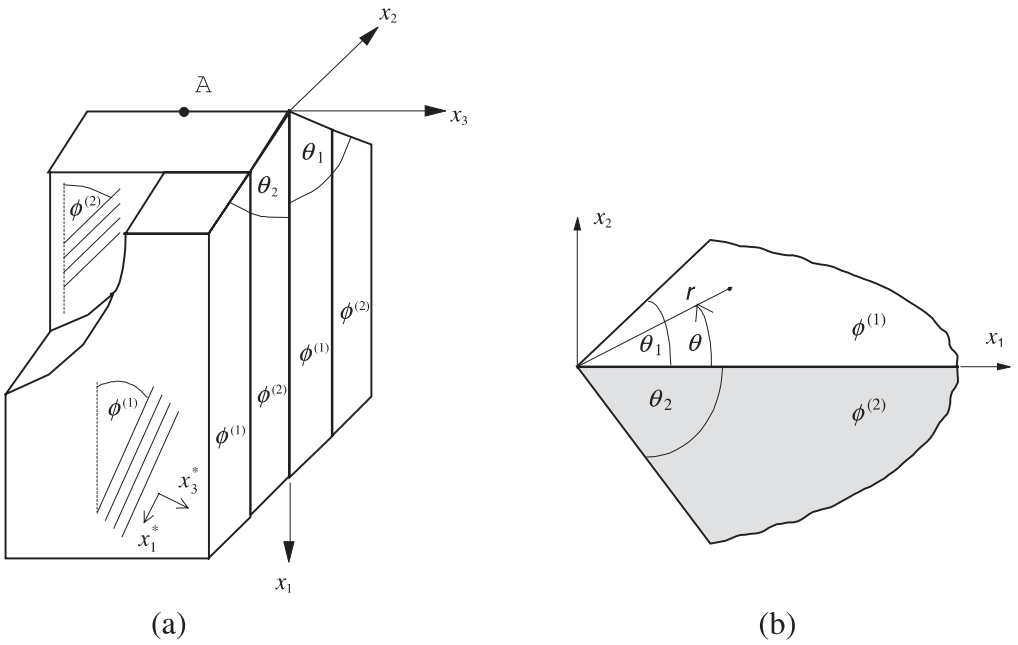

Fig. 4. (a) An angle-ply bimaterial wedge and (b) cross-sectional plane through A.

$$[m] = \begin{bmatrix} \cos^2\phi^{(N)} & 0 & \sin^2\phi^{(N)} & 0 & \sin 2\phi^{(N)} & 0 \\ 0 & 1 & 0 & 0 & 0 & 0 \\ \sin^2\phi^{(N)} & 0 & \cos^2\phi^{(N)} & 0 & -\sin 2\phi^{(N)} & 0 \\ 0 & 0 & 0 & \cos\phi^{(N)} & 0 & -\sin\phi^{(N)} \\ -(\sin 2\phi^{(N)})/2 & 0 & (\sin 2\phi^{(N)})/2 & 0 & \cos 2\phi^{(N)} & 0 \\ 0 & 0 & 0 & \sin\phi^{(N)} & 0 & \cos\phi^{(N)} \end{bmatrix}. \tag{75}$$

The roots of Eqs. (34) and (40) satisfying the condition $0 < \mathrm{Re}(k) < 1$ are obtained by using IMSL subroutine ZANLY (IMSL, 1990). It is found that the singularity is identical for the composite wedge with $(\phi^{(1)}/\phi^{(2)})$ and the composite wedge with $(-\phi^{(1)}/-\phi^{(2)})$. Similar observations were reported for two bonded quarter planes by Zwiers et al. (1982) and for a crack normal to the interface by Ting and Hoang (1984). Hence, the results presented in Tables 1–5 are for $-90° \leqslant \phi^{(1)} \leqslant 75°$ and $0° \leqslant \phi^{(2)} \leqslant 90°$.

Table 1
Angle-ply bimaterial wedge: free-edge of a graphite/epoxy laminate ($\theta_1 = \theta_2 = \pi/2$), variation of singularity with $\phi^{(1)}$ and $\phi^{(2)}$ for a fully bonded interface

$\phi^{(2)}$ (deg)	$\phi^{(1)}$											
	−90°	−75°	−60°	−45°	−30°	−15°	0°	15°	30°	45°	60°	75°
0	0.0334	0.0328	0.0287	0.0206	0.0105	0.0027	–	0.0027	0.0105	0.0206	0.0287	0.0328
15	0.0294	0.0303	0.0296	0.0250	0.0173	0.0089	0.0027	–	0.0037	0.0134	0.0234	0.0292
30	0.0199	0.0229	0.0268	0.0270	0.0234	0.0173	0.0105	0.0037	–	0.0044	0.0137	0.0202
45	0.0097	0.0131	0.0203	0.0256	0.0270	0.0250	0.0206	0.0134	0.0044	–	0.0038	0.0095
60	0.0026	0.0047	0.0117	0.0203	0.0268	0.0296	0.0287	0.0234	0.0137	0.0038	–	0.0020
75	0.0001	0.0006	0.0047	0.0131	0.0229	0.0303	0.0328	0.0292	0.0202	0.0095	0.0020	–
90	–	0.0001	0.0026	0.0097	0.0199	0.0294	0.0334	0.0294	0.0199	0.0097	0.0026	0.0001

Table 2
Angle-ply bimaterial wedge: free-edge of a graphite/epoxy laminate ($\theta_1 = \theta_2 = \pi/2$), variation of singularity with $\phi^{(1)}$ and $\phi^{(2)}$ for a frictional interface with $\mu = +0.5$

$\phi^{(2)}$ (deg)	$\phi^{(1)}$											
	−90°	−75°	−60°	−45°	−30°	−15°	0°	15°	30°	45°	60°	75°
0	–	–	–	–	–	–	–	–	–	–	–	–
15	–	–	–	–	–	0.0089	0.0122	–	–	–	–	–
30	–	–	–	–	0.0234	0.0443	0.0448	0.0302	–	–	–	–
45	–	–	–	0.0256	0.0693	0.0895	0.0897	0.0754	0.0461	–	–	–
60	–	–	0.0117	0.0663	0.1092	0.1303	0.1330	0.1217	0.0951	0.0508	–	–
75	–	0.0006	0.0306	0.0820	0.1253	0.1491	0.1556	0.1473	0.1224	0.0790	0.0283	–
90	–	0.0033	0.0310	0.0805	0.1246	0.1504	0.1585	0.1504	0.1246	0.0805	0.0310	0.0033

Table 3
Angle-ply bimaterial wedge: 90° broken graphite/epoxy laminate ($\theta_1 = \pi/2$, $\theta_2 = \pi$), variation of singularity with $\phi^{(1)}$ and $\phi^{(2)}$ for a fully bonded interface

$\phi^{(2)}$ (deg)	$\phi^{(1)}$											
	−90°	−75°	−60°	−45°	−30°	−15°	0°	15°	30°	45°	60°	75°
0	0.0439	0.0446	0.0496	0.0617	0.0812	0.1043	0.1165	0.1043	0.0812	0.0617	0.0496	0.0446
	0.3333	0.3692	0.3824	0.3748	0.3607	0.3431	0.3333	0.3431	0.3607	0.3748	0.3824	0.3692
	0.3962	0.3975	0.4138	0.4299	0.4387	0.4427	0.4438	0.4427	0.4387	0.4299	0.4138	0.3975
15	0.0467	0.0469	0.0509	0.0617	0.0795	0.1025	0.1203	0.1145	0.0914	0.0691	0.0544	0.0478
	0.3201	0.3523	0.3636	0.3562	0.3428	0.3271	0.3191	0.3333	0.3604	0.3833	0.3918	0.3575
	0.4054	0.4111	0.4307	0.4467	0.4550	0.4568	0.4531	0.4447	0.4326	0.4165	0.4000	0.4049
30	0.0550	0.0550	0.0584	0.0688	0.0862	0.1095	0.1312	0.1315	0.1090	0.0835	0.0655	0.0567
	0.2942	0.3284	0.3451	0.3384	0.3233	0.3048	0.2921	0.3029	0.3333	0.3598	0.3630	0.3318
	0.4223	0.4271	0.4435	0.4592	0.4686	0.4719	0.4695	0.4612	0.4473	0.4305	0.4203	0.4216
45	0.0686	0.0684	0.0719	0.0830	0.1011	0.1247	0.1479	0.1505	0.1286	0.1016	0.0812	0.0708
	0.2715	0.3084	0.3307	0.3255	0.3087	0.2875	0.2705	0.2769	0.3062	0.3333	0.3387	0.3095
	0.4381	0.4411	0.4537	0.4682	0.4781	0.4827	0.4824	0.4770	0.4660	0.4508	0.4392	0.4375
60	0.0832	0.0834	0.0882	0.1013	0.1215	0.1455	0.1657	0.1632	0.1405	0.1147	0.0951	0.0851
	0.2663	0.3048	0.3302	0.3251	0.3064	0.2832	0.2661	0.2745	0.3023	0.3274	0.3333	0.3051
	0.4494	0.4512	0.4607	0.4739	0.4837	0.4888	0.4898	0.4867	0.4788	0.4662	0.4538	0.4494
75	0.0909	0.0917	0.0987	0.1149	0.1377	0.1616	0.1751	0.1654	0.1420	0.1180	0.1003	0.0921
	0.2944	0.3330	0.3574	0.3509	0.3305	0.3070	0.2943	0.3061	0.3310	0.3528	0.3591	0.3333
	0.4546	0.4557	0.4636	0.4760	0.4858	0.4911	0.4927	0.4907	0.4847	0.4741	0.4617	0.4552
90	0.0918	0.0928	0.1005	0.1178	0.1416	0.1651	0.1761	0.1651	0.1416	0.1178	0.1005	0.0928
	0.3333	0.3695	0.3903	0.3831	0.3643	0.3435	0.3333	0.3435	0.3643	0.3831	0.3903	0.3695
	0.4554	0.4562	0.4639	0.4764	0.4860	0.4914	0.4930	0.4914	0.4860	0.4764	0.4639	0.4562

For the free-edge laminate problem, where the wedge angles $\theta_1 = \theta_2 = \pi/2$ (Fig. 3a), the order of singularity is given in Table 1 by varying the ply angles $\phi^{(1)}$ and $\phi^{(2)}$. For the fully bonded and frictional interfaces, either there may exist one real root or there will be no root of k. For the case of fully bonded interface, due to geometric considerations, k is identical for $(\phi^{(1)}/\phi^{(2)})$ and $(-\phi^{(2)}/-\phi^{(1)})$ wedges. This is because when the $(\phi^{(1)}/\phi^{(2)})$ wedge is flipped about the x_1-axis, and the $(-\phi^{(2)}/-\phi^{(1)})$ wedge is obtained. The singularity k does not exist when $\phi^{(1)} = \phi^{(2)}$, owing to the absence of a discontinuity, i.e., no actual interface. The singularity obtained here agrees with that of the corresponding $(\phi^{(1)}/\phi^{(2)})$ wedge reported by

Table 4
Angle-ply bimaterial wedge: 90° broken graphite/epoxy laminate ($\theta_1 = \pi/2$, $\theta_2 = \pi$), variation of singularity with $\phi^{(1)}$ and $\phi^{(2)}$ for a frictional interface with $\mu = +0.5$

$\phi^{(2)}$ (deg)	$\phi^{(1)}$											
	−90°	−75°	−60°	−45°	−30°	−15°	0°	15°	30°	45°	60°	75°
0	0.3333	0.3696	0.3917	0.3853	0.3648	0.3430	0.3333	0.3430	0.3648	0.3853	0.3917	0.3696
15	0.3257	0.3628	0.3861	0.3800	0.3593	0.3368	0.3258	0.3345	0.3565	0.3778	0.3848	0.3624
30	0.3058	0.3444	0.3697	0.3640	0.3427	0.3188	0.3061	0.3141	0.3369	0.3595	0.3671	0.3436
45	0.2819	0.3215	0.3488	0.3435	0.3216	0.2966	0.0264	0.2902	0.3138	0.3374	0.3452	0.3205
							0.2824					
60	0.2704	0.3101	0.3379	0.3326	0.3104	0.0227	0.0527	0.0257	0.3041	0.3278	0.3351	0.3093
						0.2849	0.2707	0.2797				
75	0.2947	0.3336	0.3593	0.3533	0.3311	0.0379	0.0659	0.0390	0.3296	0.3522	0.3587	0.3334
						0.3066	0.2947	0.3054				
90	0.3333	0.3696	0.3920	0.3860	0.3657	0.0405	0.0677	0.0405	0.3657	0.3860	0.3920	0.3696
						0.3435	0.3333	0.3435				

Table 5
Angle-ply bimaterial wedge: 90° broken graphite/epoxy laminate ($\theta_1 = \pi/2$, $\theta_2 = \pi$), variation of singularity with $\phi^{(1)}$ and $\phi^{(2)}$ for a frictional interface with $\mu = -0.5$

$\phi^{(2)}$ (deg)	$\phi^{(1)}$											
	−90°	−75°	−60°	−45°	−30°	−15°	0°	15°	30°	45°	60°	75°
0	0.3333	0.3430	0.3790	0.3985	0.3972	0.3697	0.3333	0.3697	0.3972	0.3985	0.3790	0.3430
	0.3853	0.3862	±0.003*i*	±0.016*i*	0.4306	0.4501	0.4520	0.4501	0.4306	±0.016*i*	±0.003*i*	0.3862
15	0.3275	0.3294	0.3468	0.3700	0.3803	0.3621	0.3264	0.3657	0.4109	0.3956	0.3756	0.3492
	0.3830	0.3912	0.4022	0.4181	0.4393	0.4498	0.4506	0.4468	±0.015*i*	±0.033*i*	±0.027*i*	0.3724
30	0.3102	0.3088	0.3231	0.3452	0.3598	0.3444	0.3076	0.3501	0.4015	0.3858	0.3652	0.3371
	0.3788	0.3902	0.4043	0.4218	0.4397	0.4467	0.4471	0.4417	±0.022*i*	±0.040*i*	±0.033*i*	0.3631
45	0.2858	0.2853	0.2998	0.3222	0.3377	0.3214	0.2837	0.3270	0.3886	0.3725	0.3517	0.3066
	0.3765	0.3871	0.4012	0.4188	0.4363	0.4431	0.4435	0.4382	±0.008*i*	±0.036*i*	±0.023*i*	0.3668
60	0.2720	0.2746	0.2913	0.3148	0.3286	0.3093	0.2712	0.3128	0.3514	0.3648	0.3207	0.2868
	0.3762	0.3838	0.3957	0.4123	0.4314	0.4406	0.4412	0.4374	0.4107	±0.013*i*	0.3677	0.3721
75	0.2949	0.3014	0.3227	0.3488	0.3570	0.3331	0.2948	0.3343	0.3650	0.3711	0.3337	0.3057
	0.3763	0.3802	0.3877	0.4014	0.4250	0.4389	0.4402	0.4378	0.4177	0.3799	0.3772	0.3761
90	0.3333	0.3435	0.3741	0.3932	0.4016	0.3698	0.3333	0.3698	0.4016	0.3932	0.3741	0.3435
	0.3763	0.3765	±0.013*i*	±0.020*i*	0.4147	0.4381	0.4400	0.4381	0.4147	±0.020*i*	±0.013*i*	0.3765

Zwiers et al. (1982). In the case of a frictional interface, the coefficient of friction is selected as $\mu = 0.5$. Due to geometric considerations, the singularity of the $(\phi^{(1)}/\phi^{(2)})$ wedge with $\mu = +\mu_0$ is identical to the singularity of the $-(\phi^{(2)}/-\phi^{(1)})$ wedge with $\mu = -\mu_0$. Hence, the singularity presented in Table 2 is for $\mu = +0.5$, i.e., the upper layer slipping to the right relative to the lower layer. The most severe singularity occurs for the (0°/90°) wedge. By comparing Tables 1 and 2, it can be observed that, if the singular stress occurs, the singularity in the case of a frictional interface with $\mu = +0.5$ is more severe than the singularity in the case of a fully bonded interface.

For the broken laminate problem, the wedge angles $\theta_1 = \pi/2$ and $\theta_2 = \pi$ (Fig. 3b). Three real roots of k exist in the range $0 < \mathrm{Re}(k) < 1$ in the case of fully bonded interface as shown in Table 3. The most severe singularity occurs for the (0°/90°) wedge and the least severe singularity occurs for the (90°/0°) wedge.

In addition, it can be observed that 0.3333 is always a root of k for $(0°/0°)$, $(90°/90°)$, $(0°/90°)$ and $(90°/0°)$ wedges. In the case of frictional interface, the coefficient of friction $\mu = \pm 0.5$ and the roots of k are presented in Tables 4 and 5. Table 4 shows that one or two real roots of k exist when the broken layer slips to the right, relative to the lower half-plane for $\mu = +0.5$, whereas Table 5 shows that there always exist two roots of k when the broken layer slips to the left, relative to the lower half-plane for $\mu = -0.5$. These two roots are either real or complex conjugates. The singularity for $\mu = -0.5$, is in general, less severe than when $\mu = +0.5$. Compared to the singularity at the free-edge of laminates, the singular stress for the broken laminate is more severe.

The variation of k for an inclined broken laminate (Fig. 3c) is investigated by keeping the wedge angle $\theta_2 = \pi$, and varying the wedge angle θ_1. In many applications, $\phi^{(1)}$ and $\phi^{(2)}$ differ by $\pi/2$ and hence, in this study, the $(\phi^{(1)}/\phi^{(2)})$ combinations considered are $(0°/90°)$, $(30°/-60°)$, $(60°/-30°)$, $(90°/0°)$, $(-60°/30°)$ and $(-30°/60°)$. As noted before, since the singularity is identical for $(\phi^{(1)}/\phi^{(2)})$ and $(-\phi^{(1)}/-\phi^{(2)})$ wedges, the numerical results are shown in Figs. 5–7, only for $(0°/90°)$, $(30°/-60°)$, $(60°/-30°)$ and $(90°/0°)$ wedges, in which the real parts of the complex conjugate roots are shown in dashed lines.

In the case of a fully bonded interface, the results presented in Fig. 5 shows that no complex root of k exists for θ_1 approximately less than 150°; two real roots exist for θ_1 approximately less than 70° and three real roots exist in the remaining range. In the range, where θ_1 is greater than 150°, one real root and two complex conjugate roots are obtained. For the interface crack problem, i.e., $\theta_1 = 180°$, the three roots of k are 0.5 and $0.5 \pm \varsigma i$ and agree with those presented by Ting (1986) and Suo (1990).

In the case of a frictional interface, the results for the wedge slipping to the right relative to the lower half-plane for $\mu = +0.5$ and for the wedge slipping to the left relative to the lower half-plane for $\mu = -0.5$ are presented in Figs. 6 and 7, respectively. The figures show that the roots of k can be either one real root, two real roots or two complex conjugate roots. For an interface crack problem, i.e., $\theta_1 = 180°$, two real roots or two complex conjugate roots exist. The first case occurs for $(0°/90°)$ and $(90°/0°)$ composites,

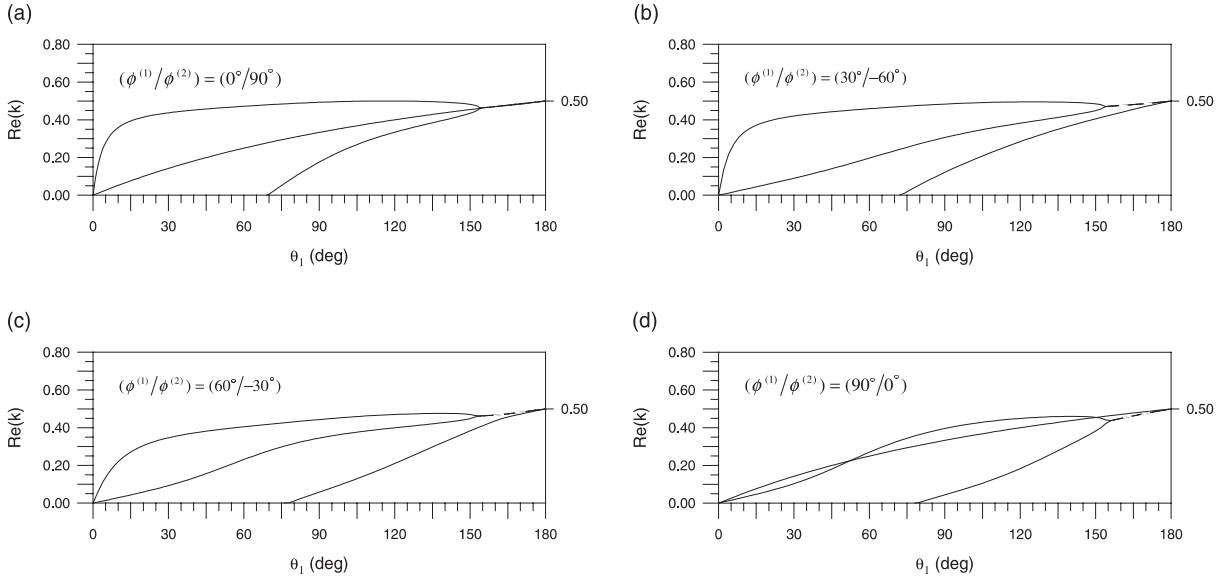

Fig. 5. Angle-ply bimaterial wedge – order of singularity for an inclined broken graphite/epoxy laminate ($\theta_2 = \pi$), for a fully bonded interface: (—) k is real and, (- - -) k is complex.

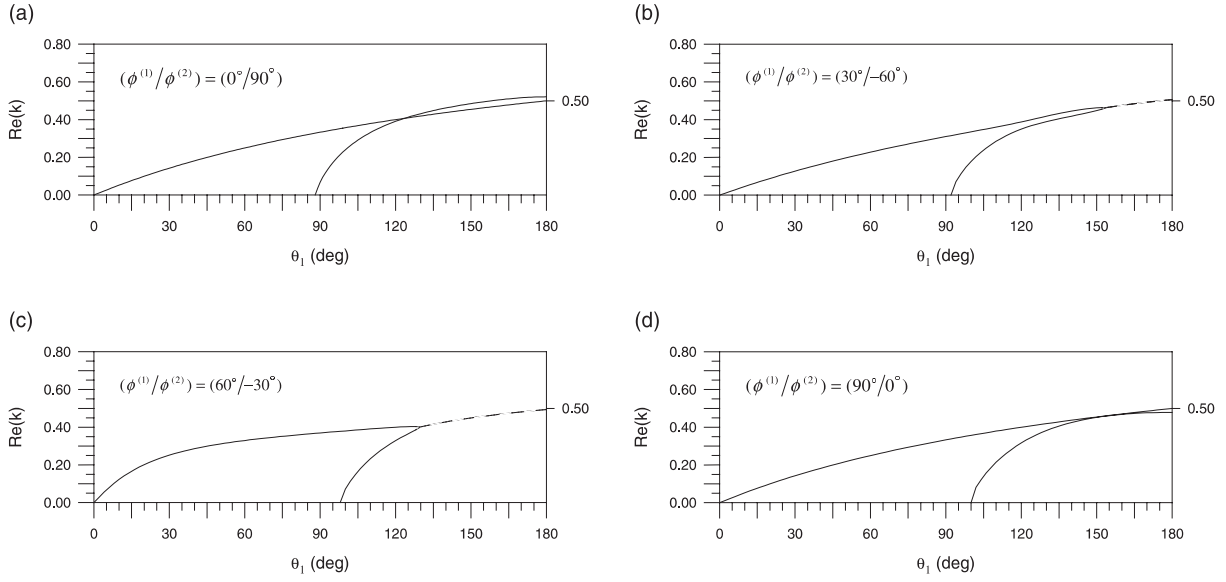

Fig. 6. Angle-ply bimaterial wedge – order of singularity for an inclined broken graphite/epoxy laminate ($\theta_2 = \pi$), for a frictional interface with $\mu = +0.5$: (—) k is real and, (- - -) k is complex.

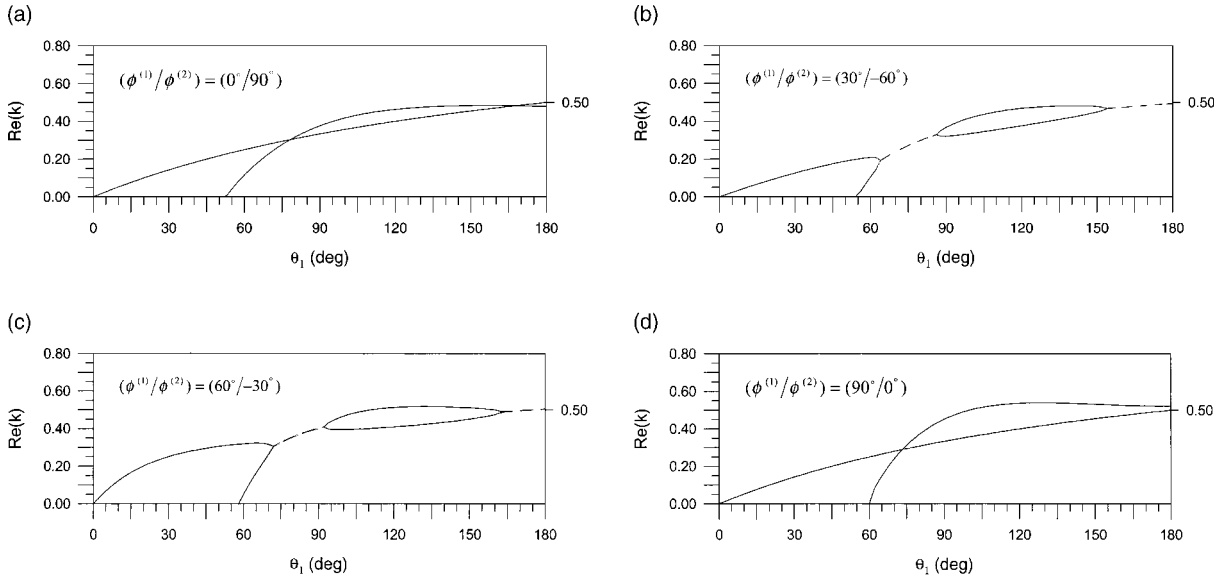

Fig. 7. Angle-ply bimaterial wedge – order of singularity for an inclined broken graphite/epoxy laminate ($\theta_2 = \pi$), for a frictional interface with $\mu = -0.5$: (—) k is real and, (- - -) k is complex.

whereas the latter case occurs for $(30°/-60°)$ and $(60°/-30°)$ composites. In addition, due to geometric considerations, the crack-tip singularity for the $(\phi^{(1)}/\phi^{(2)})$ composite with $\mu = +\mu_0$ is identical to the crack-tip singularity for the $(\phi^{(2)}/\phi^{(1)})$ composite with $\mu = -\mu_0$. By contrast to an interface crack along a fully bonded interface, in the case of an interface crack along a frictional interface, $\mathrm{Re}(k)$ can be greater than 0.5.

It can also be observed from Figs. 5a–7a for (0°/90°) wedge and Figs. 5d–7d for (90°/0°) wedge that there exists one root of k, which is identical for both the cases of fully bonded and frictional interfaces. This root corresponds to the antiplane problem, because for (0°/90°) and (90°/0°) wedges, the problems associated with inplane and antiplane deformation are uncoupled.

5.2. A monoclinic bimaterial wedge with a frictional interface

The order of singularity corresponding to the inplane deformation for a particular monoclinic bimaterial wedge consisting of a graphite/epoxy fiber reinforced composite but with different alignments of the fibers is investigated. As shown in Fig. 8, the x_1^*-axis is in the longitudinal direction of the fibers and the x_3^*-axis is normal to the cross-sectional plane and coincides with the x_3-axis of the global coordinate system, such that the x_2^*-axis is normal to the fiber direction and lies in the cross-sectional plane. The angles $\phi^{(1)}$ and $\phi^{(2)}$ denote, respectively, the fiber directions in materials 1 and 2 and are measured from the x_1-axis in the counterclockwise direction. The engineering properties of the graphite/epoxy fiber-reinforced composite referred to the (x_1^*, x_2^*, x_3^*) coordinate system are given in Eq. (71). For the $\phi^{(N)}$ material, the global coordinates are related to the local coordinates by

$$\begin{Bmatrix} x_1 \\ x_2 \\ x_3 \end{Bmatrix} = \begin{bmatrix} \cos\phi^{(N)} & -\sin\phi^{(N)} & 0 \\ \sin\phi^{(N)} & \cos\phi^{(N)} & 0 \\ 0 & 0 & 1 \end{bmatrix} \begin{Bmatrix} x_1^* \\ x_2^* \\ x_3^* \end{Bmatrix}, \quad N = 1, 2. \tag{76}$$

The stiffness matrices $C_{mn}^{(N)}$ are obtained by using Eq. (74), however, now the transformation matrix is replaced by

$$[m] = \begin{bmatrix} \cos^2\phi^{(N)} & \sin^2\phi^{(N)} & 0 & 0 & 0 & -\sin 2\phi^{(N)} \\ \sin^2\phi^{(N)} & \cos^2\phi^{(N)} & 0 & 0 & 0 & \sin 2\phi^{(N)} \\ 0 & 0 & 1 & 0 & 0 & 0 \\ 0 & 0 & 0 & \cos\phi^{(N)} & \sin\phi^{(N)} & 0 \\ 0 & 0 & 0 & -\sin\phi^{(N)} & \cos\phi^{(N)} & 0 \\ (\sin 2\phi^{(N)})/2 & -(\sin 2\phi^{(N)})/2 & 0 & 0 & 0 & \cos 2\phi^{(N)} \end{bmatrix}. \tag{77}$$

The order of singularity k can be obtained in a manner similar to that presented for an angle-ply bimaterial wedge. However, since only the inplane deformation is considered, the size of the matrix $\mathbf{K}^f$ in Eq. (39) is 4×4, as mentioned in Section 4. The three problems considered for numerical calculations are (1) the two quarter planes pressing against each other ($\theta_1 = \theta_2 = \pi/2$); (2) the quarter plane pressing on the half-plane

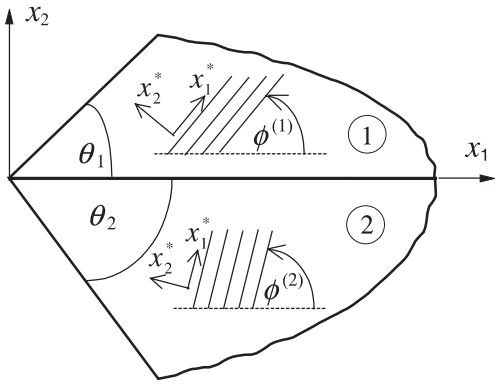

Fig. 8. A bimaterial wedge consisting of fiber-reinforced composites.

($\theta_1 = \pi/2$, $\theta_2 = \pi$), and (3) the wedge pressing on the half-plane ($\theta_2 = \pi$). The coefficient of friction μ is selected as 0.5.

For the two quarter planes pressing against each other ($\theta_1 = \theta_2 = \pi/2$), due to geometric considerations, the singularity for the $(\phi^{(1)}/\phi^{(2)})$ wedge with $\mu = +\mu_0$ is identical to the singularity for the $(-\phi^{(2)}/-\phi^{(1)})$ wedge with $\mu = -\mu_0$. Hence, the results presented in Table 6 are only for $\mu = +0.5$. The results reveal that either one real root exists or there are no roots for the selected wedge.

For the quarter plane pressing on the half-plane ($\theta_1 = \pi/2$, $\theta_2 = \pi$), the orders of singularity are presented in Tables 7 and 8. In $\mu = +0.5$, i.e., the wedge slipping to the right relative to the half-plane, there may exist one real root, two complex conjugate roots or no root of k. For $\mu = -0.5$, i.e., the wedge slipping to the left relative to the half-plane, only one real root exists for all $(\phi^{(1)}/\phi^{(2)})$ wedges. It is observed from Tables 7 and 8 that the stress singularity for $\mu = +0.5$ is less severe than for $\mu = -0.5$. In addition, if $\phi^{(2)}$ is prescribed, the most severe singular stress will occur when $\phi^{(1)} = 90°$.

Table 6
Monoclinic bimaterial wedge: two graphite/epoxy quarter planes pressing against each other ($\theta_1 = \theta_2 = \pi/2$), variation of singularity with $\phi^{(1)}$ and $\phi^{(2)}$ for a frictional interface with $\mu = +0.5$

$\phi^{(2)}$ (deg)	$\phi^{(1)}$											
	−90°	−75°	−60°	−45°	−30°	−15°	0°	15°	30°	45°	60°	75°
−90	–	–	–	–	–	–	–	0.1385	0.1683	0.1909	0.2239	0.2360
−75	–	–	–	–	–	–	–	–	0.0680	0.0906	0.1036	–
−60	–	–	–	–	–	–	–	–	–	0.0212	–	–
−45	–	–	–	–	–	–	–	–	–	–	–	–
−30	–	–	–	–	–	–	–	–	–	0.0146	–	–
−15	–	–	–	–	–	–	–	–	0.0445	0.0579	0.0579	–
0	–	–	–	–	–	–	–	0.0997	0.1244	0.1384	0.1518	0.1415
15	0.1511	–	–	–	–	–	0.1093	0.1795	0.1962	0.2116	0.2332	0.2408
30	0.1968	0.0434	–	–	–	0.0389	0.1447	0.2081	0.2227	0.2387	0.2629	0.2753
45	0.2031	0.0505	0.0061	–	0.0062	0.0454	0.1497	0.2121	0.2265	0.2426	0.2672	0.2804
60	0.2021	0.0430	–	–	–	0.0386	0.1464	0.2119	0.2270	0.2440	0.2703	0.2851
75	0.1863	–	–	–	–	–	0.1251	0.2045	0.2226	0.2423	0.2739	0.2933

Table 7
Monoclinic bimaterial wedge: a graphite/epoxy quarter plane pressing on a graphite/epoxy half-plane ($\theta_1 = \pi/2$, $\theta_2 = \pi$), variation of singularity with $\phi^{(1)}$ and $\phi^{(2)}$ for a frictional interface with $\mu = +0.5$

$\phi^{(2)}$ (deg)	$\phi^{(1)}$											
	−90°	−75°	−60°	−45°	−30°	−15°	0°	15°	30°	45°	60°	75°
−90	0.0003 $\pm 0.502i$	–	–	–	–	–	–	–	–	–	–	–
−75	0.0036 $\pm 0.528i$	–	–	–	–	–	–	–	–	–	–	–
−60	–	–	–	–	–	–	–	–	–	–	–	–
−45	–	–	–	–	–	–	–	–	0.0332	0.0579	0.0577	–
−30	–	–	–	–	–	–	–	0.0447	0.1013	0.1250	0.1479	0.1160
−15	–	–	–	–	–	–	–	0.1107	0.1475	0.1705	0.2004	0.2033
0	–	–	–	–	–	–	–	0.1435	0.1731	0.1956	0.2276	0.2395
15	–	–	–	–	–	–	–	0.1521	0.1801	0.2023	0.2347	0.2484
30	–	–	–	–	–	–	–	0.1383	0.1690	0.1915	0.2232	0.2340
45	–	–	–	–	–	–	–	0.0990	0.1388	0.1620	0.1909	0.1897
60	–	–	–	–	–	–	–	0.0222	0.0876	0.1115	0.1313	0.0759
75	–	–	–	–	–	–	–	–	0.0149	0.0399	0.0280	–

Table 8
Monoclinic bimaterial wedge: a graphite/epoxy quarter plane pressing on a graphite/epoxy half-plane ($\theta_1 = \pi/2$, $\theta_2 = \pi$), variation of singularity with $\phi^{(1)}$ and $\phi^{(2)}$ for a frictional interface with $\mu = -0.5$

$\phi^{(2)}$ (deg)	$\phi^{(1)}$											
	−90°	−75°	−60°	−45°	−30°	−15°	0°	15°	30°	45°	60°	75°
−90	0.5728	0.5065	0.4520	0.4343	0.4292	0.4044	0.3424	0.2934	0.2969	0.3566	0.4612	0.5528
−75	0.5640	0.5060	0.4549	0.4380	0.4332	0.4100	0.3529	0.3099	0.3161	0.3732	0.4667	0.5449
−60	0.5546	0.5054	0.4586	0.4426	0.4381	0.4169	0.3658	0.3294	0.3380	0.3912	0.4722	0.5370
−45	0.5475	0.5049	0.4617	0.4467	0.4425	0.4231	0.3769	0.3457	0.3556	0.4051	0.4763	0.5313
−30	0.5431	0.5046	0.4639	0.4495	0.4455	0.4272	0.3842	0.3562	0.3667	0.4135	0.4787	0.5280
−15	0.5415	0.5044	0.4647	0.4505	0.4466	0.4288	0.3871	0.3602	0.3709	0.4166	0.4796	0.5268
0	0.5425	0.5045	0.4642	0.4499	0.4459	0.4278	0.3853	0.3577	0.3683	0.4147	0.4790	0.5275
15	0.5462	0.5048	0.4623	0.4475	0.4433	0.4242	0.3789	0.3486	0.3588	0.4075	0.4770	0.5303
30	0.5527	0.5053	0.4594	0.4436	0.4392	0.4185	0.3686	0.3335	0.3425	0.3949	0.4733	0.5354
45	0.5618	0.5059	0.4557	0.4390	0.4343	0.4115	0.3558	0.3144	0.3212	0.3775	0.4680	0.5429
60	0.5711	0.5064	0.4525	0.4350	0.4300	0.4054	0.3443	0.2965	0.3006	0.3598	0.4623	0.5512
75	0.5760	0.5067	0.4510	0.4331	0.4279	0.4025	0.3389	0.2879	0.2903	0.3507	0.4592	0.5558

For the wedge pressing on the half-plane ($\theta_2 = \pi$), the influence of θ_1 on the singularity k is investigated for (0°/90°), (30°/ − 60°), (60°/ − 30°), (90°/0°), (−60°/30°) and (−30°/60°) wedges and the results are presented in Fig. 9. In the case of the wedge slipping to the left relative to the half-plane ($\mu = -0.5$), no root of k exists for θ_1 approximately less than 50°, but there always exist one real root for the remaining range. Similarly, in the case of the wedge slipping to the right relative to the lower half-plane ($\mu = +0.5$), no root of k exists for θ_1 approximately less than 90°, but one real root exists for the remaining range. The singularity for $\mu = -0.5$ is generally more severe than for $\mu = +0.5$. For an interface crack, i.e. $\theta_1 = 180°$, the order of singularity is 0.5 for both relative slip directions. This agrees with Eq. (54) as the composite considered has $\beta = 0$.

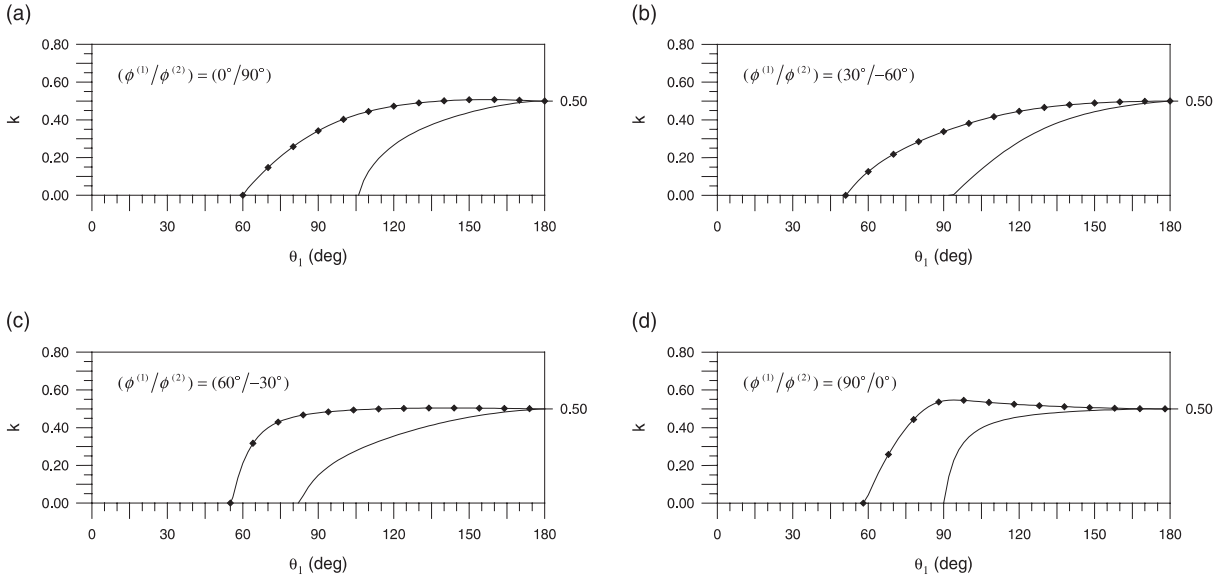

Fig. 9. Monoclinic bimaterial wedge – order of singularity for a graphite/epoxy wedge pressing on a graphite/epoxy half-plane ($\theta_2 = \pi$), along a frictional interface: (—) $\mu = +0.5$ and, (—◆—) $\mu = -0.5$.

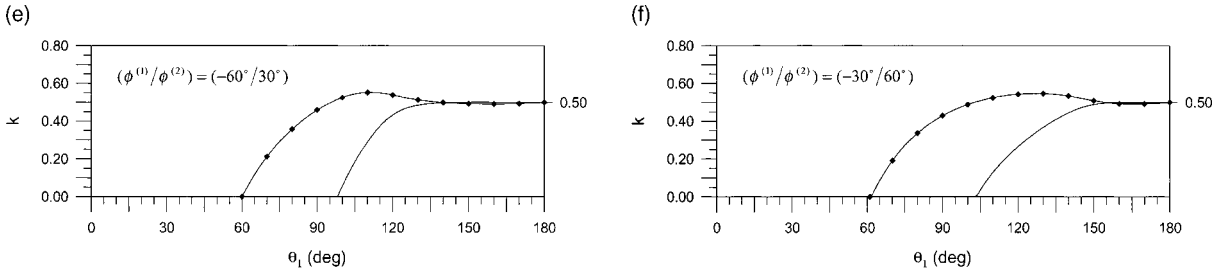

Fig. 9. (*continued*)

Acknowledgements

The first author gratefully acknowledges the scholarship provided by the Japanese Government to the Asian Institute of Technology, which enabled him to complete his D. Eng. studies.

References

Auld, B.A., 1973. Acoustic Fields and Waves in Solids, vol. 1. Wiley, New York.

Barnett, D.M., Lothe, J., 1973. Synthesis of the sextic and the integral formalism for dislocations, Greens functions, and surface waves in anisotropic elastic solids. Physica Norvegica 7, 13–19.

Bogy, D.B., 1968. Edge-bonded dissimilar orthogonal elastic wedges under normal and shear loading. ASME Journal of Applied Mechanics 35, 460–466.

Bogy, D.B., 1970. On the problem of edge-bonded elastic quarter-planes loaded at the boundary. International Journal of Solids and Structures 6, 1287–1313.

Bogy, D.B., 1971. Two edge-bonded elastic wedges of different materials and wedge angles under surface tractions. ASME Journal of Applied Mechanics 38, 377–386.

Bogy, D.B., 1972. The plane solution for anisotropic elastic wedges under normal and shear loading. ASME Journal of Applied Mechanics 39, 1103–1109.

Bogy, D.B., Wang, K.C., 1971. Stress singularities at interface corners in bonded dissimilar isotropic elastic materials. International Journal of Solids and Structures 7, 993–1005.

Christensen, R.M., 1979. Mechanics of Composite Materials. Wiley, New York.

Comninou, M., 1976. Stress singularity at a sharp edge in contact problems with friction. Journal of Applied Mathematics and Physics 27, 493–499.

Delale, F., 1984. Stress singularities in bonded anisotropic materials. International Journal of Solids and Structures 20, 31–40.

Dempsey, J.P., Sinclair, G.B., 1979. On the stress singularities in plane elasticity of the composite wedge. Journal of Elasticity 9, 373–391.

Dundurs, J., Lee, M.-S., 1972. Stress concentration at a sharp edge in contact problems. Journal of Elasticity 2, 109–112.

Eshelby, J.D., Read, W.T., Shockley, W., 1953. Anisotropic elasticity with applications to dislocation theory. Acta Metallurgica 1, 251–259.

Gdoutos, E.E., Theocaris, P.S., 1975. Stress concentrations at the apex of a plane indenter acting on an elastic half-plane. ASME Journal of Applied Mechanics 42, 688–692.

Green, A.E., Zerna, W., 1954. Theoretical Elasticity. Clarendon Press, Oxford, U.K.

Hein, L., Erdogan, F., 1971. Stress singularities in a two-material wedge. International Journal of Fracture Mechanics 7, 317–330.

IMSL, 1990. IMSL FORTRAN Subroutine for Mathematical Applications. IMSL, Math/Library, Version 2.0. Houston, TX.

Kalandiia, A.L., 1969. Remarks on the singularity of elastic solutions near corners. Journal of Applied Mathematics and Mechanics 33, 127–131.

Kim, T.W., Im, S., 1995. Boundary layers in wedges of laminated composite strips under generalized plane deformation; part I asymptotic solutions. International Journal of Solids and Structures 32, 609–628.

Kuo, M.C., Bogy, D.B., 1974a. Plane solutions for the displacement and traction-displacement problems for anisotropic elastic wedges. ASME Journal of Applied Mechanics 41, 197–202.

Kuo, M.C., Bogy, D.B., 1974b. Plane solutions for traction problems on orthotropic unsymmetrical wedges and symmetrically twinned wedges. ASME Journal of Applied Mechanics 41, 203–208.

Lekhnitskii, S.G., 1950. Theory of Elasticity of an Anisotropic Elastic Body. Gostekhizdat, Moscow (in Russian). Theory of Elasticity of an Anisotropic Elastic Body. Holden-Day, San Francisco (in English, 1963) and Mir Publication, Moscow (in English, 1981).

Lin, Y.Y., Sung, J.C., 1998. Stress singularities at the apex of a dissimilar anisotropic wedge. ASME Journal of Applied Mechanics 65, 454–463.

Oh, H-S, Babuška, I., 1998. The method of auxiliary mapping for the finite element solutions of elasticity problems containing singularities. Journal of Computational Physics 121, 193–212.

Poonsawat, P., Wijeyewickrema, A.C., Karasudhi, P., 1998. Singular stress fields of an anisotropic composite wedge with a frictional interface. ASCE 12th Engineering Mechanics Conference, La Jolla, San Diego, CA, 578–581.

Stroh, A.N., 1958. Dislocations and cracks in anisotropic elasticity. Philosophical Magazine 3, 625–646.

Suo, Z., 1990. Singularities, interfaces and cracks in dissimilar anisotropic media. Proceedings of the Royal Society of London, 331–358, A427.

Szabó, B.A., Babuška, I., 1991. Finite Element Analysis. Wiley, New York.

Ting, T.C.T., 1986. Explicit solutions and invariance of the singularities at an interface crack in anisotropic composites. International Journal of Solids and Structures 22, 965–983.

Ting, T.C.T., 1995. Generalized Dundurs constants for anisotropic bimaterials. International Journal of Solids and Structures 32, 483–500.

Ting, T.C.T., 1996. Anisotropic Elasticity; Theory and Applications. Oxford University Press, New York.

Ting, T.C.T., Chou, S.C., 1981. Edge singularities in anisotropic composites. International Journal of Solids and Structures 17, 1057–1068.

Ting, T.C.T., Hoang, P.H., 1984. Singularities at the tip of a crack normal to the interface of an anisotropic layered composite. International Journal of Solids and Structures 20, 439–454.

Wang, S.S., Choi, I., 1982. Boundary-layer effects in composite laminates; part I free-edge stress singularities; part II free-edge stress solutions and characteristics. ASME Journal of Applied Mechanics 49, 541–550.

Williams, M.L., 1952. Stress singularities resulting from various boundary conditions in angular corners of plates in extension. ASME Journal of Applied Mechanics 19, 526–528.

Zwiers, R.L., Ting, T.C.T., Spilker, R.L., 1982. On the logarithmic singularity of free edge stress in laminated composites under uniform extension. ASME Journal of Applied Mechanics 49, 562–569.